Calculating Radiation Emitted by Laser-Driven Relativistic Electrons

Christoph Schulzke

A senior thesis submitted to the faculty of
Brigham Young University
in partial fulfillment of the requirements for the degree of

Bachelor of Science

Justin Peatross and Michael Ware, Advisors

Department of Physics and Astronomy

Brigham Young University

2 January 2019

ABSTRACT

Calculating Radiation Emitted by Laser-Driven
Relativistic Electrons

Christoph Schulzke
Department of Physics and Astronomy, BYU
Bachelor of Science

Electrons driven by intense laser fields exhibit nonlinear Thomson scattering. Measuring these radiation patterns has become of interest to many groups including our group at Brigham Young University.The theoretical description of this phenomenon was outlined by Sarachik and Schappert in 1970. The solution for the scattered light involves a numeric integral. They developed an approximation which uses a series of Bessel functions in place of the integral. In this thesis we investigate the efficacy of the Bessel-series approximation to see if gives an advantage over the numerical-integration approach. We find only a modest advantage for certain parameters. Generally, performing the integration numerically is a sensible approach.

Keywords: nonlinear optics, Thompson scattering

ACKNOWLEDGMENTS

I would like to thank the generous donors of Brigham Young University for providing the funds needed for me to perform this research. Without them I would have been overwhelmed with responsibilities.

I would also like to mention the contribution of Dr. Michael Ware. His mentorship in my first few semesters was considerable and impactful.

Lastly, I must thank Dr. Justin Peatross for his critical support in this research. He has made an enormous time investment in me and my research. Without his guidance and instruction none of this would have been possible.

Contents

Chapter 1

Electron in a Laser Field

With the invention of the laser in the 1960's, a new regime of light-matter interactions became available to researchers. Within a decade, researchers began theoretical investigations of super-intense laser fields acting on charged particles [1, 2], many years in advance of laser technologies reaching the field strengths studied. At sufficiently high laser power, a free electron in a laser field can undergo relativistic motion in response to the oscillating light field.

Ignoring radiation reaction, the momentum $\vec{p}$ of the particle is governed by the Lorentz force law

$$\frac{d\vec{p}}{dt} = q(\vec{E} + \vec{u} \times \vec{B}) \tag{1.1}$$

where q is the particle charge, $\vec{u}$ is its velocity, $\vec{E}$ is the electric field of the laser, and $\vec{B}$ the laser's magnetic field. At low intensities, the magnetic contribution is usually ignored. This greatly reduces the complexity of the equation. However, if the particle moves relativistically, the magnetic field becomes as important as the electric field. Additionally, at these intensities, a factor of γ must be included in the definition of $\vec{p}$ such that

$$\vec{p} = m\vec{u}\gamma \tag{1.2}$$

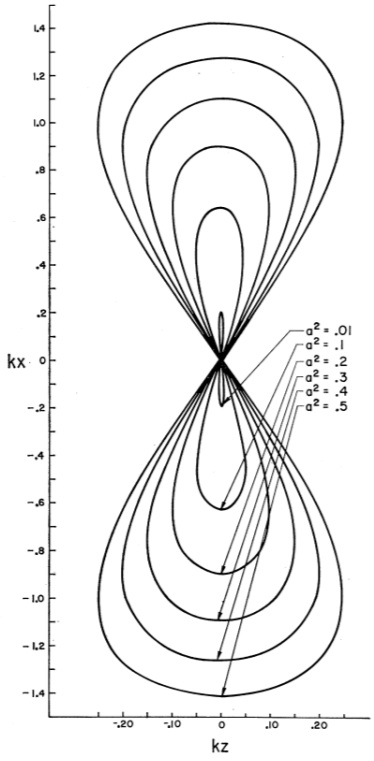

Figure 1.1 The figure-8 trajectory motion taken from E. S. Sarachik and G. T. Schappert, Phys. Rev. D **1** , 2738-2753 (1970). The larger figure-8 corresponds to a stronger laser field. The path is for plane wave linearly polarized aligned vertically in the plane of the page and propagating to the right.

where

$$\gamma = \frac{1}{\sqrt{1-u^2/c^2}} \tag{1.3}$$

Since both γ and $\vec{u}$ depend on t, we have to use the product rule on the left hand side. This, in addition to the cross product on the right hand side, yields a nonlinear equation which requires the aid of a computer in order to solve.

In 1970, two researchers at NASA, Sarachik and Schappert, [2] solved the above equations for an electron in a plane-wave electromagnetic field. The full solution involves an integral that needs to be solved using numerical methods. The derivation of this solution is discussed in Chapter 2. They developed an analytic expression, in the average rest frame of the electron, for the the

figure-8-shaped path of the electron trajectory. As the laser power increases, the length of one lap around the path approaches the wavelength of the driving plane wave. This corresponds to the electron approaching the speed of light.

Even though the path shape looks symmetric, the electron trajectory is rather asymmetric. The position of the electron along the path as a function of time does not have an analytic solution. The electron spends more time on one half of the figure-8 than the other. Moreover, electron moves to the right on both the top and bottom of the figure 8 and moves to the left on the left on both the vertical parts. This asymmetry has implication for the radiation.

1.1 Nonlinear Thomson Scattering

Having solved for the electron trajectory, Sarachik and Schappert also worked out a formula for the radiation emitted by the electron, [2] Because the relativistic motion of the electron is not a simple sinusoid, it contains harmonic components of the driving field, both odd and even. The harmonics represent a nonlinear form of Thomson scattering. Sarachik and Schappert developed an integral expression for the harmonic components of the scattered light in the far field. The integral cannot be solved analytically, however, so numerical methods are required to get any results. This is straight forward today with the aid of computers, but in 1970 if presented a formidable challenge.

Sarachik and Schappert were able to perform the integral analytically after representing part of the integrand as an infinite series of Bessel functions. By truncating the series, it is possible to arrive at an approximation to the solution. However, without the help of a computer, there is not a practical means of checking the reliability of their approximation. The details of this approximation and its accuracy is the subject of this thesis.

Figures 1.2 and 1.3 show calculated polarization-resolved scattered radiation patterns of nonlinear Thomson scattering according to the theory by Sarachik and Schappert.

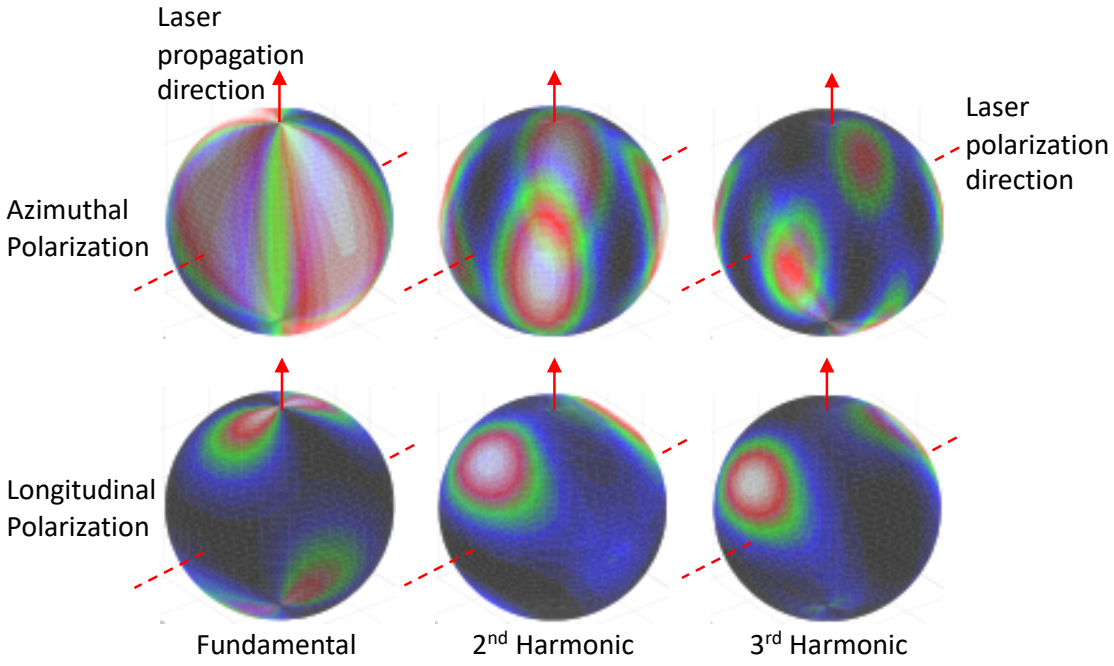

Figure 1.2 Calculated azimuthal (top) and longitudinal (bottom) polarization components of the fundamental, second harmonic, and third harmonic of Thomson scattering in the far field. Electrons are stimulated by linearly-polarized 800 nm light at 1.5×10^{18} W/cm^2 and $\lambda = 800$ nm..

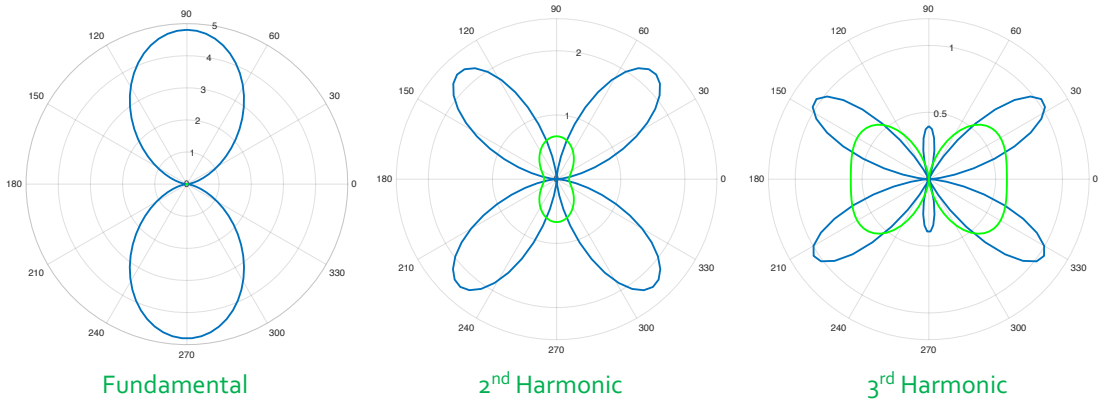

Figure 1.3 Calculated azimuthal (green) and longitudinal (blue) polarization components of the fundamental, second harmonic, and third harmonic of Thomson scattering in the plane of the 'equator' in Fig. 1.2.

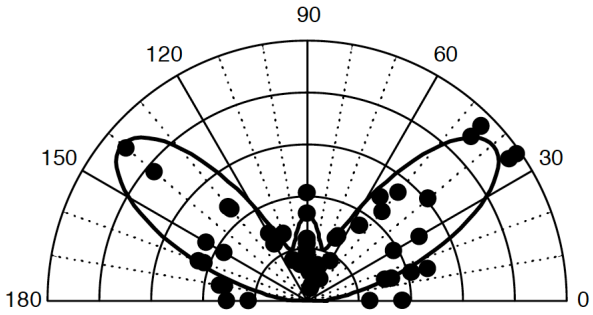

Figure 1.4 Measured and calculated third harmonic emission taken from Chen et al., Nature **396** , 653-655 (1998). The graph plots intensity in various directions perpendicular to the laser beam out the side of the focus.

1.2 Measurements

In 1998, the group of Don Umstadter, while at the University of Nebraska, experimentally measured second and third harmonic light scattered from free electrons in an intense laser focus and compared it with the predictions of Sarachik and Schappert. [3]. They traced the shape of the the far-field radiation distribution out the side of the laser focus. Their measured third-harmonic data is shown in Fig. 1.4. More recently, the Umstadter group at the University of Nebraska-Lincoln's Extreme Light Laboratory, measured Thomson scattering for relativistic electrons colliding with laser pulses at extraordinary intensities. The highly nonlinear interaction produces a beam of hard x-rays. The principles remain the same in this extreme nonlinear reaction involving many orders of harmonics.

Our group at BYU is interested in measuring polarization-resolved nonlinear Thomson scattering from electrons in an intense laser focus. Previous experiments measured the total light scattering for both polarization components, whereas we will be attempting to measure both curves for each harmonic as shown in Fig. 1.3. For the new experiments, we are using a femtosecond pulsed laser capable of reaching modestly relativistic intensities in the 10^{18}/W/cm^2 range. Measuring the polarization requires the addition of a polarizer attached to a rotating stage to the experimental setup. The added dimension of information that polarization carries can be associated with different features in the figure-8 electron trajectory.

1.3 Thesis Overview

For my senior-thesis project, I checked the accuracy and usefulness of the Bessel approximation outlined by Sarachik and Schappert. The approximation is an alternative approach to calculating emission such as that shown in Figs. 1.2 and 1.3. My objective is to compare the approximation to numerically computing the integral. I found that the usefulness of the approximation depends on the power of the laser, the harmonic order, and the number of terms that need to be included in the series for accuracy. In chapter 2, I provide a derivation of the electron trajectory and its scattered radiation. In chapter 3, I describe the Bessel-series approximation and assess its performance,

Chapter 2

Motion and Radiation of Relativistic Electrons

2.1 Solving the Lorentz Force Law

As was mentioned, the solution to Eqs. (1.1)-(1.3) for an incident plane wave was first described in a paper by Sarachik and Schappert in 1970 [2]. Their work established the now well-known figure-8 trajectory of a charged particle within a laser field as shown in Fig. 1.1. They developed their solution using the Hamilton-Jacobi formalism, which employs the vector potential. Instead, here we follow the approach of Hartemann et al. [4], who worked directly with Eqs. (1.1)-(1.3).

To aid in solving the equations, we first develop an expression for $\frac{d\gamma}{dt}$. To do this, we take the dot product of the velocity with the force equation, which eliminates the cross product with the magnetic field and gives the compact expression

$$\vec{u} \cdot \frac{d}{dt}\vec{u}\gamma = \frac{q}{m}\vec{u} \cdot \vec{E} \tag{2.1}$$

$$\Rightarrow \frac{d\gamma}{dt} = \frac{q}{mc^2}\vec{u} \cdot \vec{E} \tag{2.2}$$

To solve for the motion of the particle, we must first pick electric and magnetic fields. For the purposes of this paper we pick a uniform plane wave with arbitrary elliptical polarization:

$$\vec{E} = E_0(\phi)\left[\hat{x}\sqrt{1-\delta^2}\cos\phi + \hat{y}\delta\sin\phi\right] \tag{2.3}$$

$$\vec{B} = \frac{E_0(\phi)}{c}\left[-\hat{x}\delta\sin\phi + \hat{y}\sqrt{1-\delta^2}\cos\phi\right] \tag{2.4}$$

These fields obey Maxwell's equations inasmuch as the field envelope $E_0(\phi)$ varies slowly. The dimensionless parameter δ ranges from -1 to 1 and determines the ellipticity of the field. A value of $\delta = 1$ results in y-polarized light, $\delta = 0$ yields x-polarized light, and $\delta = \pm\frac{1}{\sqrt{2}}$ gives circularly polarized light. The variable ϕ is phase of the laser given by $\phi = kz - \omega t$.

Substituting these electric and magnetic fields into our force equation and performing the dot and cross products gives us a system of three coupled differential equations:

$$\frac{d}{dt}\gamma u_x = \frac{qE_0(\phi)}{m}\sqrt{1-\delta^2}\left(1-\frac{u_z}{c}\right)\cos\phi \tag{2.5}$$

$$\frac{d}{dt}\gamma u_y = \frac{qE_0(\phi)}{m}\delta\left(1-\frac{u_z}{c}\right)\sin\phi \tag{2.6}$$

$$\frac{d}{dt}\gamma u_z = \frac{qE_0(\phi)}{m}\left(\sqrt{1-\delta^2}\cos\phi\frac{u_x}{c} + \delta\sin\phi\frac{u_y}{c}\right) \tag{2.7}$$

An interesting result is obtained when we subtract Eq. (2.7) from Eq. (2.2). After rearranging the result we arrive at the fact that $\gamma\left(1-\frac{u_z}{c}\right)$ is constant with respect to time, since its time derivative is zero. Thus,

$$\gamma\left(1-\frac{u_z}{c}\right) = \gamma_0\left(1-\frac{u_{z0}}{c}\right) \tag{2.8}$$

The subscript "0" indicates the initial value of the variable. This allows us to write the z component of velocity as a function of only γ and initial conditions.

We are now in a position to solve the equation of motion for the charged particle in a uniform laser field. We will need the time derivative of the laser phase which is easily obtained by taking the derivative of the definition of the phase $\phi = \frac{\omega}{c}z - \omega t$ to get $\frac{d\phi}{dt} = \frac{\omega}{c}u_z - \omega$. We can now write the equation as a derivative of ϕ instead of t. If we assume that the field envelope, $E_0(\phi)$, varies slowly

and is zero for ϕ_0, we can integrate these equations directly to arrive at the solution:

$$\frac{\vec{u}}{c} = \frac{1}{\gamma}\left[\gamma_0 \frac{\vec{u}_0}{c} - \hat{x}\alpha\sqrt{1-\delta^2}\sin\phi + \hat{y}\alpha\delta\cos\phi + \hat{z}(\gamma-\gamma_0)\right] \tag{2.9}$$

where $\alpha(\phi) \equiv \dfrac{qE_0(\phi)}{m\omega c}$. In terms of laser intensity I and wavelength, this may be written as $\alpha = \dfrac{q\lambda}{\pi mc^2}\sqrt{\dfrac{I}{2\varepsilon_0 c}}$. For 800 nm light, $\alpha = 1$ when $I = 2.1\times10^{18}$ W/cm^2.

We obtain an expression for γ by injecting Eq. (2.9) into Eq. (1.3) to obtain

$$\gamma = \gamma_0 + \frac{\alpha\left(-\sqrt{1-\delta^2}\frac{u_{x0}}{c}\sin\phi + \delta\frac{u_{y0}}{c}\cos\phi\right)}{\left(1-\frac{u_{z0}}{c}\right)} + \frac{\alpha^2\left(\left(2\delta^2-1\right)\cos 2\phi + 1\right)}{4\gamma_0\left(1-\frac{u_{z0}}{c}\right)} \tag{2.10}$$

From here, we may take a derivative to acquire the acceleration and integral to find the position:

$$\vec{a} = \frac{d\vec{u}}{dt} = \frac{d\vec{u}}{d\phi}\frac{d\phi}{dt} = -\omega\left(1-\frac{u_z}{c}\right)\frac{d\vec{u}}{d\phi} \tag{2.11}$$

$$\frac{d\vec{r}}{dt} = \frac{d\vec{r}}{d\phi}\frac{d\phi}{dt} = -\omega\left(1-\frac{u_z}{c}\right) \Rightarrow \vec{r} = -\frac{1}{\omega\gamma_0\left(1-\dfrac{u_{z0}}{c}\right)}\int_{\phi_0}^{\phi}\gamma\vec{u}d\phi' \tag{2.12}$$

2.2 Average Rest Frame

We would like to average the velocity over a period of motion T, where $2\pi = \omega(z/c - T)$. Since by definition $u_{z\text{ave}} = z/T$, this may be rewritten as $1/T = -\omega_{\text{L}}(1-u_{z\text{ave}}/c)/2\pi$. Using this together with $\dfrac{d\phi}{dt} = \dfrac{\omega}{c}u_z - \omega$ and (2.8), the velocity averaging may be expressed as $\vec{u}_{\text{ave}} = \frac{1}{T}\int_0^T \vec{u}dt = \frac{1-u_{z\text{ave}}/c}{2\pi\gamma_0(1-u_{z0}/c)}\int_0^{2\pi}\gamma\vec{u}d\phi$. All oscillatory terms in Eq. (2.9) and Eq. (2.10) vanish under this integration. The result of the averaging yields

$$\vec{u}_{\text{ave}} = \frac{\vec{u}_0 + \hat{z}c\tilde{\alpha}^2/4}{1+\tilde{\alpha}^2/4} \quad \text{where} \quad \tilde{\alpha} = \frac{\alpha}{\gamma_0\sqrt{1-u_{z0}/c}} \tag{2.13}$$

This formula shows that during the pulse, the average particle velocity is different than its initial velocity. If we chose the initial velocity of the electron correctly, we can make the average velocity be zero. This takes place in a rest frame different from the laboratory frame.

In the average rest-frame, (2.9) simplifies to

$$\frac{\gamma\vec{u}\,'}{c} = -\hat{x}'\alpha\sqrt{1-\delta^2}\sin\phi + \hat{y}'\alpha\delta\cos\phi + \hat{z}'\frac{\frac{\alpha^2}{4}\left(2\delta^2-1\right)}{\sqrt{1+\frac{\alpha^2}{2}}}\cos 2\phi \tag{2.14}$$

with $\gamma = \frac{1+\frac{\alpha^2}{2}+\frac{\alpha^2}{4}\left(2\delta^2-1\right)\cos 2\phi}{\sqrt{1+\frac{\alpha^2}{2}}}$. The position becomes

$$\vec{r}\,' = \frac{c}{\omega'}\frac{\alpha}{\sqrt{1+\frac{\alpha^2}{2}}}\left[-\hat{x}'\sqrt{1-\delta^2}\cos\phi - \hat{y}'\delta\sin\phi + \hat{z}'\left(1-2\delta^2\right)\frac{\alpha}{8\sqrt{1+\frac{\alpha^2}{2}}}\sin 2\phi\right] \tag{2.15}$$

These expressions are parameterized by ϕ. After obtaining z from (2.15) for a given phase ϕ, one can get the associated time t from $\phi = \frac{\omega}{c}z - \omega t$.

Plotting the position in this average rest frame gives us the figure-8 shaped trajectory we showed in Fig. 1.1, associated with $\delta = 0$. While appearing highly symmetrical, the particle spends more time on one half of the path than on the other. We will see this asymmetry's affect when we investigate the radiation emitted by the particle in the next section.

As the laser power increases, the speed approaches the speed of light and the length of one lap around the figure-8 approaches a wavelength. The effects of laser power are asymptotic. This asymptotic behavior will be discussed in Chapter 3 when we investigate the dependence of the Bessel approximation on laser power.

2.3 Radiation of Relativistic Electrons

An electron executing the trajectory described above has an accompanying radiation pattern. The formula for the far-field electric field radiated from a point charge is [5]

$$\vec{E} = \frac{q}{4\pi\varepsilon_0 cR}\frac{\hat{R}\times\left(\left(\hat{R}-\frac{\vec{u}}{c}\right)\times\frac{\vec{a}}{c}\right)}{\left(1-\hat{R}\cdot\frac{\vec{u}}{c}\right)^3} \tag{2.16}$$

where $\hat{R}$ is the unit vector pointing from the point charge to the detector and is evaluated at time t. Note that $\vec{u}$ and $\vec{a}$ are evaluated at the retarded time t_r, which is related through $t = t_\mathrm{r} + \left(R - \vec{r}\cdot\hat{R}\right)/c$.

In order to see the harmonic distribution, we need to take the Fourier transform of this field:

$$\vec{E}(\omega) = \frac{q}{4\pi\varepsilon_0 cR}\frac{1}{2\pi}\int_{-\infty}^{\infty}\frac{\hat{R}\times\left(\left(\hat{R}-\frac{\vec{u}}{c}\right)\times\frac{\vec{a}}{c}\right)}{\left(1-\hat{R}\cdot\frac{\vec{u}}{c}\right)^3}e^{-i\omega t}dt \tag{2.17}$$

After further manipulation and changing the integration variable to t_r, we get

$$\vec{E}(\omega) = i\omega\frac{q}{4\pi\varepsilon_0 cR}\frac{1}{\sqrt{2\pi}}\int_{-\infty}^{\infty}\hat{R}\times\left(\hat{R}\times\frac{\vec{u}}{c}\right)e^{-i\omega\left(t_r+\frac{1}{c}(R-\vec{r}\cdot\hat{R})\right)}dt_r \tag{2.18}$$

It will be more convenient to express the electric field as a function of phase ϕ. So we use the transformation

$$t_r - \frac{z}{c} = -\frac{\phi}{\omega_0} \Rightarrow dt_r = -\frac{d\phi}{\omega_0\left(1-\frac{u_z}{c}\right)} \tag{2.19}$$

where ω_0 is the angular frequency of the laser. Applying this transformation gives us

$$\vec{E}(\omega) = -ie^{-iNR\omega_0/c}\frac{q}{4\pi\varepsilon_0 cR}\frac{1}{\gamma_0\left(1-\frac{u_{z0}}{c}\right)}\frac{Nn}{\sqrt{2\pi}}\int_0^{2\pi}\hat{R}\times\left(\hat{R}\times\gamma\frac{\vec{u}}{c}\right)e^{iN\left(\phi+\omega_0(\vec{r}\cdot\hat{R}-z)/c\right)}d\phi \tag{2.20}$$

where n is the number of cycles in the pulse and N is the harmonic order. Note that

$$\hat{R}\times\left(\hat{R}\times\vec{u}\right) = \hat{\theta}\left(-u_x\cos\theta\cos\psi - u_y\cos\theta\sin\psi + u_z\sin\theta\right) + \hat{\psi}\left(u_x\sin\psi - u_y\cos\psi\right) \tag{2.21}$$

$$\vec{r}\cdot\hat{R} = x\sin\theta\cos\psi + y\sin\theta\sin\psi + z\cos\theta \tag{2.22}$$

where we use ψ as the azimuthal angle to avoid confusion with the laser phase. Using these the integral in the formula can be written as:

$$\int_0^{2\pi}\gamma\Big[\hat{\theta}\left(-u_x\cos\theta\cos\psi - u_y\cos\theta\sin\psi + u_z\sin\theta\right) + \hat{\psi}\left(u_x\sin\psi - u_y\cos\psi\right)\Big]\times \exp\Big[-iN\phi + \frac{\omega_0}{c}\left(x\sin\theta\cos\psi + y\sin\theta\sin\psi + z(\cos\theta-1)\right)\Big]d\phi \tag{2.23}$$

These formulas gives us the harmonic and polarization information of the radiation emitted by a laser driven electron. This is the formula used to produce Figs. 1.2 and 1.3. Finding an approximation for the integral in Eq. (2.23) is the subject of Chapter 3.

Chapter 3

Bessel Functions as an Approximation

3.1 Bessel Substitutions

The complex exponentials in Eq. (2.23) can be replaced with infinite series of Bessel functions. Moreover, the Bessel functions allow us to accomplish the integration analytically. Our purpose is to explore the usefulness of a truncated series to represent Eq. (2.23). Before introducing the series of Bessel functions, it is helpful to write Eq. (2.20) as

$$\vec{E}(\omega) = \hat{\theta}\left(I_x \cos\theta\cos\psi - I_y \cos\theta\sin\psi + I_z \sin\theta\right) + \hat{\psi}\left(-I_x \sin\psi - I_y \cos\psi\right) \tag{3.1}$$

where

$$\begin{aligned} I_x &= \sqrt{1-\delta^2} N\sigma \int_0^{2\pi} d\phi \sin\phi e^{-iN\phi + iN\left(a_x\cos\phi + a_y\sin\phi + a_z\sin 2\phi\right)} \\ I_y &= \delta N\sigma \int_0^{2\pi} d\phi \cos\phi e^{-iN\phi + iN\left(a_x\cos\phi + a_y\sin\phi + a_z\sin 2\phi\right)} \\ I_z &= \left(1-2\delta^2\right)\tfrac{N\sigma^2}{4} \int_0^{2\pi} d\phi \cos 2\phi e^{-iN\phi + iN\left(a_x\cos\phi + a_y\sin\phi + a_z\sin 2\phi\right)} \end{aligned} \tag{3.2}$$

and

$$\begin{aligned} a_x &= \sigma\sqrt{1-\delta^2}\cos\theta\cos\psi \\ a_y &= \sigma\delta\cos\theta\sin\psi \\ a_z &= \tfrac{\sigma^2}{8}\left(1-2\delta^2\right)\left(1-\cos\theta\right) \end{aligned} \tag{3.3}$$

with

$$\sigma = \frac{\alpha}{\sqrt{1+\alpha^2/2}} \tag{3.4}$$

We may now introduce the following identities [6]:

$$\begin{aligned} e^{i\rho cos\phi} &= \sum_{n=-\infty}^{\infty} i^n e^{in\phi} J_n(\rho) \\ e^{i\rho sin\phi} &= \sum_{n=-\infty}^{\infty} e^{in\phi} J_n(\rho) \end{aligned} \tag{3.5}$$

With these formulas, we may write the integral in I_x as

$$\int_0^{2\pi} d\phi \sin\phi e^{-iN(\phi + a_x\cos\phi + a_y\sin\phi + a_z\sin 2\phi)} = \sum_{m=-\infty}^{\infty}\sum_{l=-\infty}^{\infty}\sum_{n=-\infty}^{\infty} i^l J_n(Na_z)J_m(Na_x)J_l(Na_y)\int_0^{2\pi} d\phi \sin\phi e^{i\phi(l+m+2n-N)} \tag{3.6}$$

Fortunately, this can be simplified considerably. The integration renders zero unless the argument of the exponent is zero. This results in Kroneker delta function of the form $\delta_{l+m+2n-N+1,0}$ and $\delta_{l+m+2n-N-1,0}$. We can now write l in terms of n and m: $l = N-m-2n\pm 1$. This leaves us with a simpler formula, but we still have a product of two infinite series to deal with:

$$-i\sum_{m=-\infty}^{\infty}\sum_{n=-\infty}^{\infty} i^m J_n(Na_z)J_m(Na_x)\Big[J_{N-m-2n-1}(Na_y) - J_{N-m-2n+1}(Na_y)\Big] \tag{3.7}$$

We can collapse another of the series with the aid of the Graf addition formula [6]:

$$\sum_{n=-\infty}^{\infty} i^n J_n(z_2)J_{n+m}(z_1) = \Big[\frac{z_1+iz_2}{z_1-iz_2}\Big]^{m/2} J_m\big([z_1^2+z_2^2]^{1/2}\big) \tag{3.8}$$

Note that the paper by Sarachik and Schappert presents and employs an incorrect version of the Graf addition formula. Their left-hand side incorrectly includes a factor $(-i)^n$ in place of i^n. Using the Graf addition formula we are able to compress the two series into one. And thus arrive at a manageable formula for the radiation in terms of a sum:

$$I_x = -i\pi\sqrt{1-\delta^2}N\sigma\sum_{n=-\infty}^{\infty} J_n(Na_z)\left[\Big(\frac{a_y+ia_x}{a_y-ia_x}\Big)^{\frac{N-2n-1}{2}} J_{N-2n-1}\Big(N\sqrt{a_y^2+a_x^2}\Big) - \Big(\frac{a_y+ia_x}{a_y-ia_x}\Big)^{\frac{N-2n+1}{2}} J_{N-2n+1}\Big(N\sqrt{a_y^2+a_x^2}\Big)\right] \tag{3.9}$$

By going through the same process with the I_y and I_z portions of the radiation integral we get:

$$I_y = \pi\delta N\sigma \sum_{n=-\infty}^{\infty} J_n(Na_z)\left[\left(\frac{a_y+ia_x}{a_y-ia_x}\right)^{\frac{N-2n-1}{2}} J_{N-2n-1}\left(N\sqrt{a_y^2+a_x^2}\right) - \left(\frac{a_y+ia_x}{a_y-ia_x}\right)^{\frac{N-2n+1}{2}} J_{N-2n+1}\left(N\sqrt{a_y^2+a_x^2}\right)\right] \quad (3.10)$$

$$I_z = \pi(1-2\delta^2)\frac{N\sigma^2}{4} \sum_{n=-\infty}^{\infty} J_n(Na_z)\left[\left(\frac{a_y+ia_x}{a_y-ia_x}\right)^{\frac{N-2n-2}{2}} J_{N-2n-2}\left(N\sqrt{a_y^2+a_x^2}\right) - \left(\frac{a_y+ia_x}{a_y-ia_x}\right)^{\frac{N-2n+2}{2}} J_{N-2n+2}\left(N\sqrt{a_y^2+a_x^2}\right)\right] \quad (3.11)$$

We now have an alternate formula for the scattered radiation, which avoids integration. However, the price we pay is an infinite series of Bessel functions. However, it still requires the use of a continue for any practical implementation. The question remains as to how many terms in the infinite series are required to achieve a good approximation of the result. In referring to the order of tan approximation, we references the maxunum size of n. Note that an nth-order approximation actually has $n+1$ terms in it. This is due to the inclusion of both negative and positive values of n plus zero.

3.2 Accuracy of Approximation

The series approximation becomes more accurate as more terms are included. Hypothetically, the series can achieve greater accuracy than the numeric integral. However, this would only be useful if more accuracy is required than can be accomplished with numerical integration. Nevertheless, with relatively few terms, the series can achieve remarkable accuracy. Figures 3.1 and 3.2 show the degree of accuracy that is possible with a small number of terms. By using a number of terms equivalent to the harmonic order, one can achieve a precision of five significant figures.

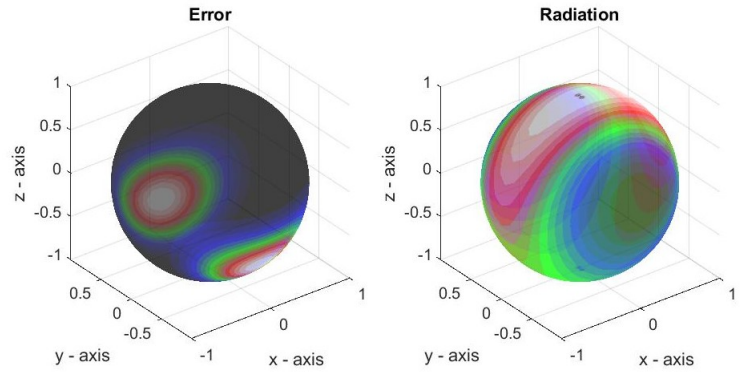

Figure 3.1 The left side shows the fractional error between the numeric integral and the Bessel series using $n_{max} = 2$ for the first harmonic. The colored areas on the sphere correspond to the angles at which the radiation would actually be detected. The red/white areas are the areas where maximum error occurs. The white represents an error of only 1.3×10^{-5}. The right side shows the radiation pattern of the first harmonic.

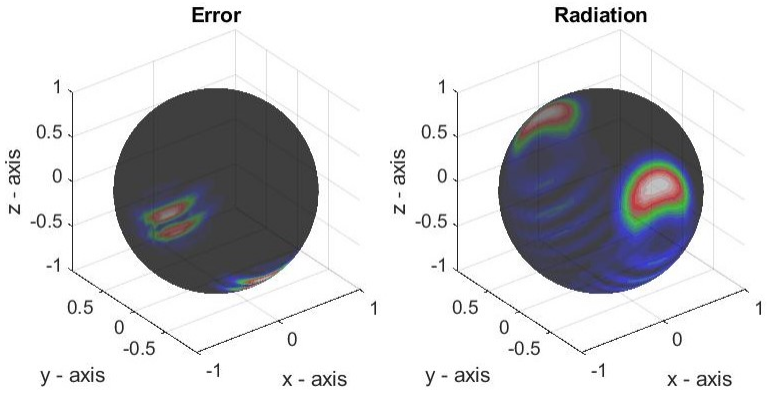

Figure 3.2 This figure is setup the same as Figure 3.1. This is for the 15th harmonic using $n_{max} = 15$ for the approximation. The maximum error is 9.44×10^{-9}.

3.3 Harmonic Order

In examining which terms in a series contribute most to scattered light for a given harmonic, there is no connection between the nth harmonic and the nth term of the approximation. The nth term does not hold any information special to the nth harmonic. The zeroth-order approximation is the most significant term for any harmonic, but it does not give a complete nor sufficient description of the radiation.

In general, to get an accurate result, you must use a nth order approximation for the nth harmonic. The actual number depends on the desired accuracy, but a 'rule of thumb' is that this number of terms ensures an accuracy to within five significant figures. The only exception to this rule appears to be the first harmonic which requires a second order approximation to get to within three significant figures.

3.4 Laser Power

The accuracy of the truncated series is effected only modestly by laser power. As can be seen in Fig. 3.3, powers corresponding to $\alpha > 20$ all have about the same accuracy. The laser at BYU has $\alpha \approx 1$. The error at high power is only one order of magnitude larger than at relatively weak power, but the approximations precision still maintains at least five significant figures. If the precision of an approximation is in doubt, more terms can always be added to the series to compensate.

At low power, as shown in Fig. 3.4, the accuracy improves. If α is on the order of 0.01 or less, the number of terms needed in the series is reduced. In this low-power limit, it is sufficient to use $\frac{N}{2}$ terms in the series, where N is the harmonic order.

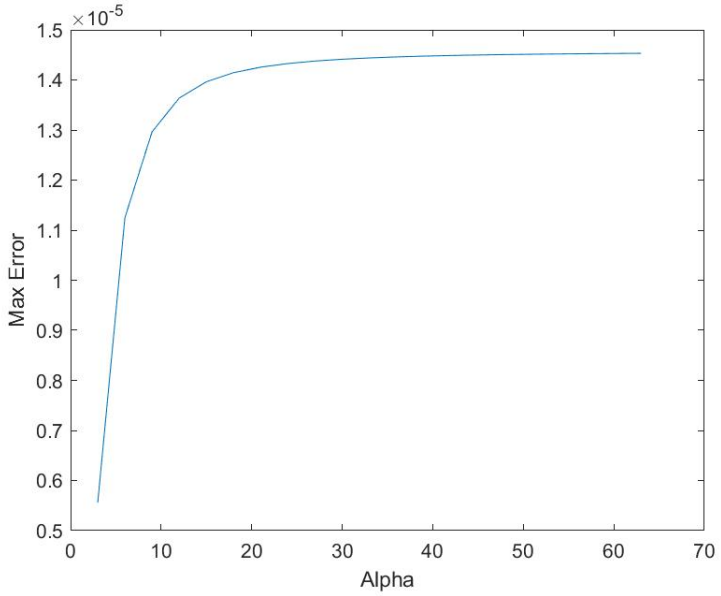

Figure 3.3 This graph shows the maximum fractional error between the Bessel series and numeric integral on the sphere as a function of α. The exact numbers are not as important as the general shape of the graph. This is for the first harmonic with two terms used in the series. As we can see, the error increases steeply, but linearly, with laser power up until $\alpha \approx 30$ where it reaches an asymptote. After this, increasing the laser power does little to increase the error.

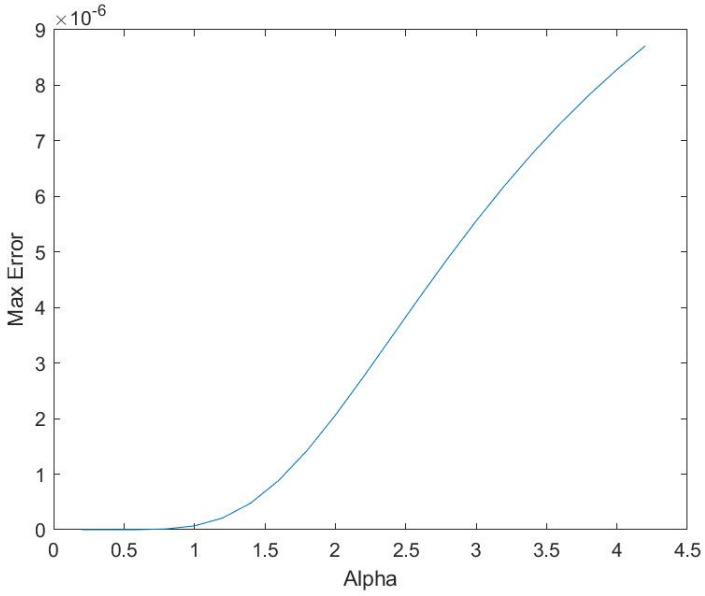

Figure 3.4 For small α, the size of the error is significantly smaller overall. The error again has an asymptote down below $\alpha \approx 0.5$. The error then exhibits the same steep linear dependence on α as it does at large values.

3.5 Computation Speed

Potentially the most useful aspect of using the Bessel series is the computation speed. Figures 3.5 and 3.6 show the computation time of the series for the 1st and 10th harmonic as a function of the number of terms included. The computation time for the numeric integral is also shown for reference. For the first harmonic, the computation time becomes equivalent when around 90 terms are included in the series, far more than necessary. As previously discussed, the series only requires a couple terms for good accuracy. For this harmonic order, the series is an order of magnitude faster than the integral. When we look at the results for the tenth harmonic, shown in Figure 3.5, we see that the equivalent computation time is reached somewhere beyond 100 terms, but again the series only requires a fraction of this for high accuracy. The computation time of the series approximation is an order of magnitude smaller than computing the integral.

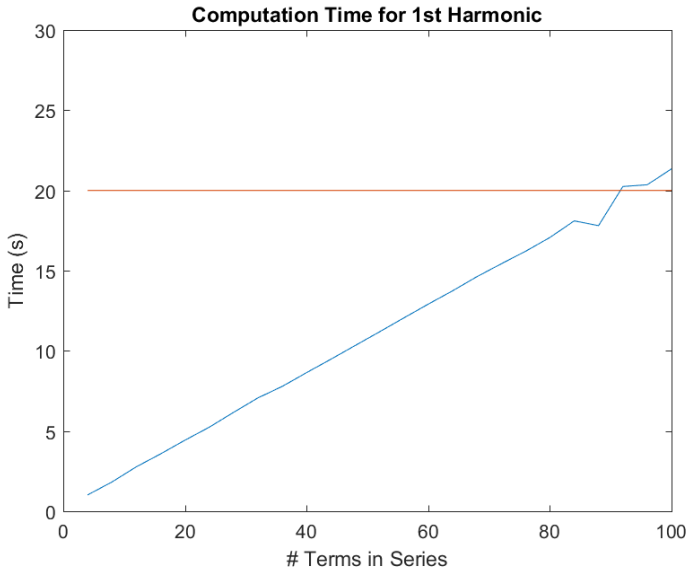

Figure 3.5 This shows the result from on average of ten runs for both the numeric integral and the series approximation for the first harmonic. The computation time of the series is plotted in blue against the number of terms included in the series. The red line shows the time required for the numeric integral.

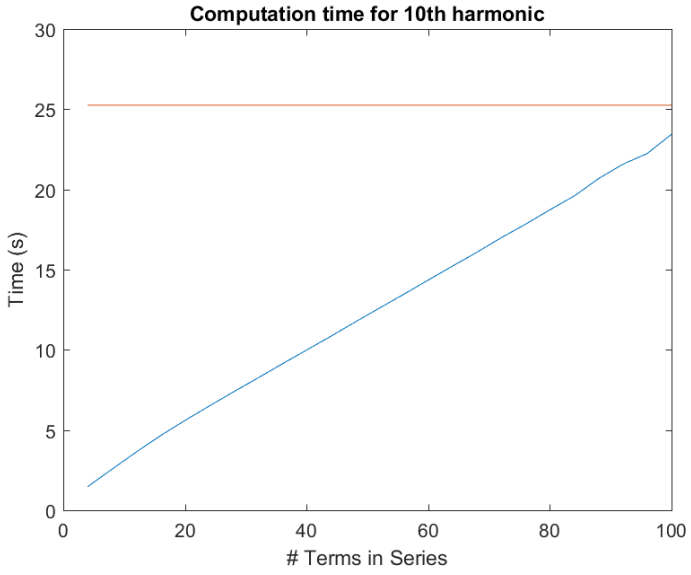

Figure 3.6 This shows the result from on average of ten runs for both the numeric integral and the series approximation for the tenth harmonic. The computation time of the series is plotted in blue against the number of terms included in the series. The red line shows the time required for the numeric integral.

3.6 Conclusion

Using the Bessel series in place of the numeric integral is a legitimate approach to calculating the radiation of an electron. The series approximation can be more cumbersome to code, however, with only modest benefit. The series approach is about an order of magnitude faster, but the integral can still be performed within a matter of seconds. The other advantage of the series approximation is the ability to achieve, in principle, very high precision. This does not seem to be a particularly compelling reason, given the adequate performance of the numeric integral. The choice of which to use is a matter of preference.

Appendix A

Code

The code for computing, comparing, and displaying the numeric integral and Bessel approximation.

```
clear; close all;
format long;
al= 10; delta = 1;
sigma=al/sqrt(1+al^2/2);
N = 30; num = 50; terms = 30;
[X,Y,Z]=sphere(num);
ct = Z;
ct(26,:) = ct(25,:)/100;
st = sqrt(1-ct.^2);
st(1,:) = st(2,:)/100;
st(num+1,:) = st(num,:)/100;
cp = X./st;
cp(1,:) = cp(2,:);
cp(num+1,:) = cp(num,:);
```

```
sp = Y./st;
sp(:,1) = sp(:,2)/100;
sp(:,26) = sp(:,25)/100;
sp(:,num+1) = sp(:,num)/100;
sp(1,:) = sp(2,:)/100;
sp(num+1,:) = sp(num,:)/100;
I=X*0; I2=I;
for j=1:num+1
 j
 for k=1:num+1
  ax=sigma*sqrt(1-delta^2)*st(j,k)*cp(j,k);
  ay=sigma*delta*st(j,k)*sp(j,k);
  az=sigma^2/8*(1-2*delta^2)*(1-ct(j,k));
% Integration approach
  fx=(@(phi)sqrt(1-delta^2)*N*sigma*sin(phi)...
      .*exp(-1i*N*phi+1i*N*(ax*cos(phi)+ay*sin(phi)+az*sin(2*phi))));
  fy=(@(phi)delta*N*sigma*cos(phi)...
      .*exp(-1i*N*phi+1i*N*(ax*cos(phi)+ay*sin(phi)+az*sin(2*phi))));
  fz=(@(phi)(1-2*delta^2)*N*sigma^2/4*cos(2*phi)...
      .*exp(1i*N*(-phi+ax*cos(phi)+ay*sin(phi)+az*sin(2*phi))));
  Ix2=integral(fx,0,2*pi);
  Iy2=integral(fy,0,2*pi);
  Iz2=integral(fz,0,2*pi);
%
  It=abs(Ix2*ct(j,k)*cp(j,k)-Iy2*ct(j,k)*sp(j,k)+Iz2*st(j,k))^2;
```

```
    Ip=abs(-Ix2*sp(j,k)-Iy2*cp(j,k))^2;
    I(j,k)=Ip+It;
% Series approach
    Ix=0; Iy=0; Iz=0;
    if delta==0
        w = 1i*sign(ax);
    elseif delta==1
        w = sign(ay);
    else
        w=(ay+1i*ax)/sqrt(ay^2+ax^2);
        % This accounts for the factor of 1/2 in w exponent
    end
    q=N*sqrt(ax^2+ay^2);
    for n=-terms:terms
     Ix=Ix-1i*pi*sqrt(1-delta^2)*N*sigma*besselj(n,N*az)*...
          (w^((N-2*n-1))*besselj(N-2*n-1,q)-w^((N-2*n+1))*besselj(N-2*n+1,q));
     Iy=Iy+pi*delta*N*sigma*besselj(n,N*az)*...
          (w^((N-2*n-1))*besselj(N-2*n-1,q)+w^((N-2*n+1))*besselj(N-2*n+1,q));
     Iz=Iz+pi*(1-2*delta^2)*N*sigma^2/4*besselj(n,N*az)*...
          (w^((N-2*n-2))*besselj(N-2*n-2,q)+w^((N-2*n+2))*besselj(N-2*n+2,q));
    end
%
    It=abs(Ix*ct(j,k)*cp(j,k)-Iy*ct(j,k)*sp(j,k)+Iz*st(j,k))^2;
    Ip=abs(-Ix*sp(j,k)-Iy*cp(j,k))^2;
    I2(j,k)=Ip+It;
```

```
 end;
end;
Ierror = abs((I2-I)/(max(max(I))));
MaxError = max(max(abs(Ierror)));

figure;
colormap([0 0 0;0 0 .25;0 0 .5;0 0 .75;0 0 1;0 .25 .75;0 .5 .5;...
    0 .75 .25;0 1 0;.25 .75 0;.5 .5 0;.75 .25 .33;...
    1 0 0;1 .25 .25;1 .5 .5;1 .75 .75;1 1 1]);
surf(X,Y,Z,Ierror,'Edgecolor', 'none')
xlabel('x - axis')
ylabel('y - axis')
zlabel('z - axis')
shading interp
axis equal
alpha(.5)
```

Bibliography

[1] J. H. Eberly and A. Sleepers,"Trajectory and Mass Shift of a Classical Electron in a Radiation Pulse," Phys. Rev. **176**, 1570-1573 (1968).

[2] E. S. Sarachik and G. T. Schappert, "Classical Theory of the Scattering of Intense Laser Radiation by Free Electrons," Phys. Rev. D **1** , 2738-2753 (1970).

[3] Chen, S. Y., Maksimchuk, A., and Umstadter, D. "Experimental observation of relativistic nonlinear Thomson scattering," Nature **396** , 653-655 (1998).

[4] F. V. Hartemann, S. N. Fochs, G. P. Le Sage, N. C. Luhmann, Jr., J. G. Woodworth, M. D. Perry, Y. J. Chen, A. K. Kerman, "Nonlinear ponderomotive scattering of relativistic electrons by an intense laser field at focus," Phys. Rev. E **51**, 4833-4843 (1995).

[5] David. J. Griffiths *Introduction of Electrodynamics*, 3rd ed., Prentice Hall (1999).

[6] Abramowitz and Stegun, *Handbook of Mathematical Functions*, 10th ed., National Bureau of Standards (1972); Formulas 9.1.81, 9.1.79, 9.1.5.